ISSN: 2250-3676
Volume-3, Issue-3, 217-223

ASYMMETRICAL FB DC-DC CONVERTER FOR FUEL CELL APPLICATIONS

Divya S[1], Sreedevi G[2]

[1] *PG Scholar, EEE Department, Govt Engineering College, Idukki, Kerala, India,* ***diyaries@gmail.com***
[2] *Assistant Professor, EEE Department, Govt Engineering College, Idukki, Kerala, India,* ***sreedevig8@yahoo.co.in***

Abstract

In the past few decades, full bridge dc-dc converters are extensively applied in medium to high power applications. In this paper, an asymmetric FB converter with high voltage gain is presented.. The converter attains high voltage gain with the voltage doubler circuit in the secondary side. The converter achieves ZVS for all power switches and ZCS for output diodes. The asymmetrical converter with high voltage gain can be used for interfacing with low voltage sources and high voltage loads like fuel cells, photovoltaic systems, uninterruptable power supplies, electric vehicles etc. Increase in energy consumption and depletion in fossil fuels have led to researches in using renewable sources of energy. One technology which can be based upon sustainable sources of energy is fuel cell. In this paper, a PEM fuel cell is modelled using Matlab/Simulink. The modelled fuel cell is interfaced with the asymmetrical converter. The paper gives the simulation of a 150 W asymmetric full bridge converter for an output voltage of 400V and input of 48V. The modelled PEM fuel cell act as the dc input source for the converter. The computer simulation the converter is done using MATLAB/SIMULINK and is interfaced with the mathematical model of fuel cell and various waveforms are presented in the paper.

Index Terms: *DC-DC converter, asymmetric duty cycle, ZVS, ZCS, PI controller, PEM fuel cell.*

----------***----------

1. INTRODUCTION

High efficiency dc-dc switching converters are widely used in each gadgets and electronic systems. They are usually used to obtain a stabilized output voltage from a given input dc voltage which is lower from that input voltage, or higher or generic. There are different types of dc-dc converters like buck, boost, full bridge, push-pull, forward converter and each day a new topology is being proposed by researchers. These converters with high voltage gain are used to interface between low voltage sources to high voltage load side. Thus high voltage gain dc to dc converters find application in photovoltaic systems, fuel cells, electric vehicles, UPS etc[1]. A conventional boost converter is often used in step-up applications due to its simple structure and low cost. However, it is not suitable for high step-up applications. This is because the conventional boost converter requires an extreme duty cycle to obtain high-voltage gain and its voltage gain is limited due to its parasitic components [2]. In order to remedy these problems, high step-up dc–dc converters using coupled inductors were introduced. Thus many topologies with dc- dc converter with isolation transformer, current fed converters, ZVS and ZCS converters, asymmetrical converters etc have been developed over the years.

In asymmetrical full bridge dc to dc converter a clamping capacitor was connected in series with the two switching legs of the full bridge, this makes asymmetric voltage distribution across switches in the two legs of the full bridge converter. The inductor in primary or a series inductor in secondary is used to obtain ZVS for main switches [3]. The asymmetrical pulse width modulation (APWM) technique was introduced in [4]. The APWM technique has various advantages such as zero switching loss, no conduction loss penalty, and fixed switching frequency. The phase shifted PWM technique can be used for asymmetrical converters and asymmetrical phase shifted converters [5]. This technique helps in reducing the switching losses in converters and decreases peaking of the reverse diode voltage. An asymmetric full bridge converter with high voltage gain is introduced in [6]. The high voltage gain is obtained by proper switching of the switches. Apart from that, the converter consists of a voltage doubler circuit in the secondary side helping in having high voltage across the load side. Asymmetrical PWM technique is used for switching all the switches of the converter. The proposed converter achieves ZVS for all power switches and ZCS for output diodes.

The dc to dc converters can be used to interface between fuel cells, photovoltaic systems, and electric vehicles. In the highly energy concerned world, focus has been shifted to utilise renewable sources of energy. This has motivated to interface the asymmetrical full bridge converter with a low voltage source and this has resulted in focusing to fuel cells. Fuel cells are electrochemical devices that convert the chemical energy of a gaseous fuel directly into electricity. Among the several types of fuel cells, classified by the type of electrolyte material being used, the Proton Exchange Membrane (PEM) FC and the Solid Oxide Fuel Cell (SOFC) are commonly used in power generation applications. PEM

ISSN: 2250-3676
Volume-3, Issue-3, 217-223

based fuel cells are more popular. In order to study the performance of the fuel cell when used as a source for a dc-dc converter, the mathematical model of the fuel cell is required. There exist many mathematical models representing PEM fuel cell [7]-[9].

In this paper an asymmetrical full bridge converter with high voltage gain interfaced with fuel is proposed. The converter achieves zero voltage switching for the power switches and zero current switching for the output diodes. A 150W asymmetric FB dc-dc converter is simulated using Matlab/Simulink and its various waveforms are discussed.

2. FULL BRIDGE ASYMMETRIC CONVERTER WITH HIGH VOLTAGE GAIN

The circuit diagram of the converter with high-voltage gain is shown in fig 1. The converter has four power switches S_1 through S_4. There is a clamping capacitor C_c between top side switches S_1 and S_3 of two switch bridges[6]. The voltages across the switches S_1 and S_2 in the first bridge are confined to the input voltage V_{in}. The clamping capacitor C_c can clamp the voltages across the switches S_3 and S_4 in the second bridge and to $V_{in}+V_c$. The output stage of the proposed converter has a voltage doubler structure that consists of the secondary winding N_2 of the transformer T, the serial inductor L_s, the output capacitors C_{o1}, and C_{o2}, and the output diodes D_{o1} and D_{o2}.

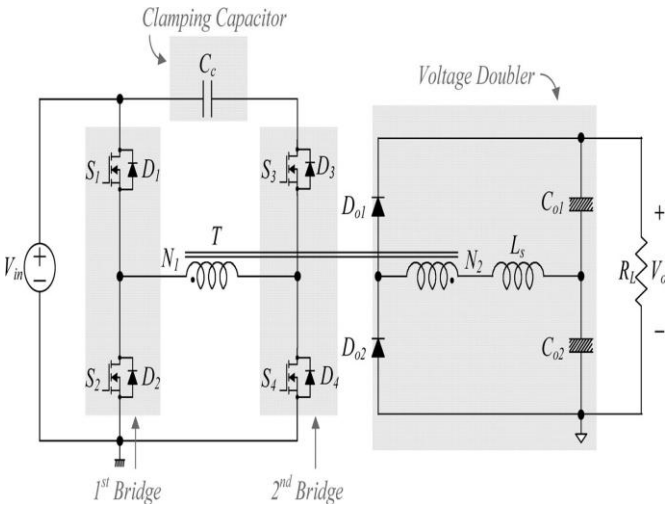

Fig -1: Circuit diagram

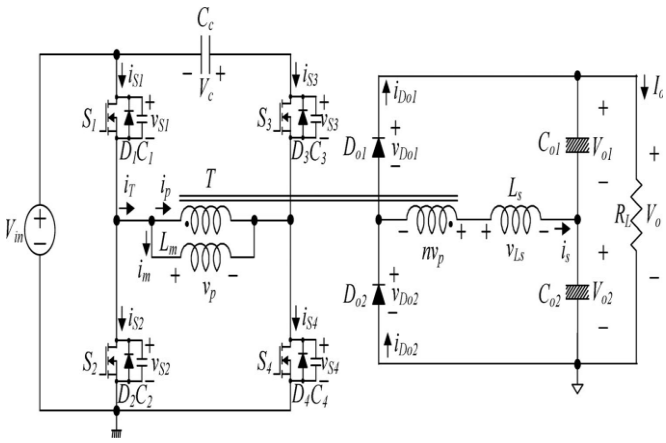

Fig -2: Equivalent circuit diagram

In the voltage doubler structure, the voltage gain increases and the voltage stresses of the output diodes are confined to the output voltage V_o without any auxiliary circuits. The equivalent circuit of the proposed converter is shown in fig. 2. The diodes D_1 through D_4 are the intrinsic body diodes of all switches. The capacitors C_1 through C_4 represent their parasitic output capacitances. The transformer T is modeled as the magnetizing inductance L_m and the ideal transformer that has a turn ratio of 1:n ($n = N_2/N_1$). To simplify the analysis, it is assumed that the clamping capacitor C_c has a large value and the voltage across C_c is constant as V_c under a steady state. Similarly, the output capacitor voltages are assumed to be constant as V_{o1} and V_{o2}, respectively. The theoretical waveforms of the converter are shown in Fig 3.

ISSN: 2250-3676
Volume-3, Issue-3, 217-223

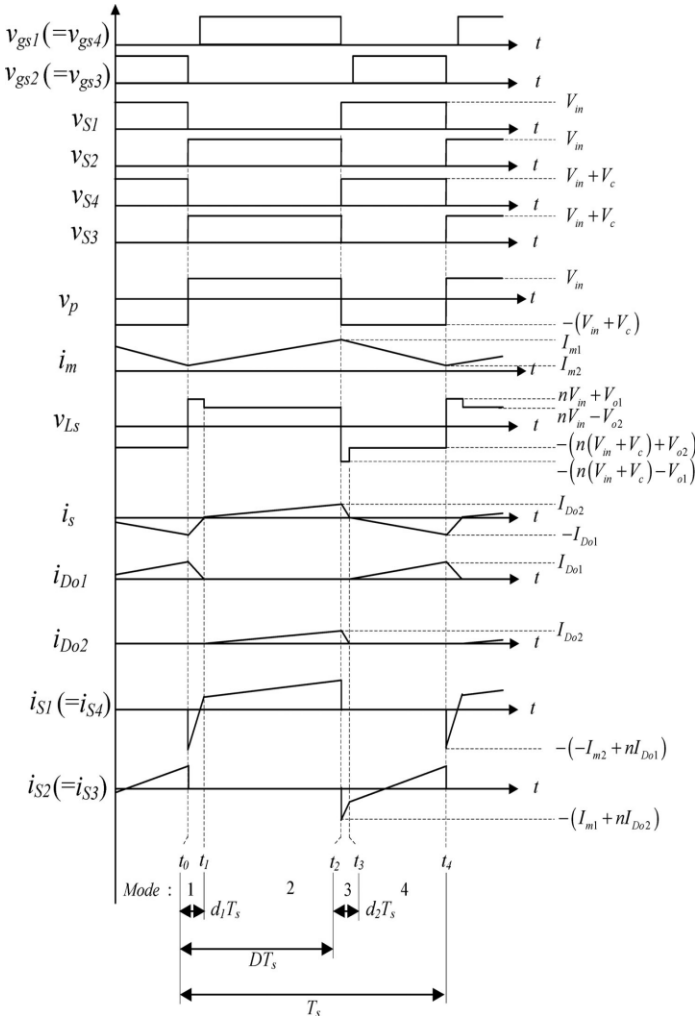

Fig -3: Theoretical waveforms

The switch S_1 (S_4) and the switch S_2 (S_3) are operated asymmetrically and the duty cycle D is based on the switch S_1 (S_4). A small delay(d_1T_s and d_2T_s) between driving signals for S_1 (S_4) and S_2 (S_3) is a deadtime for the switches. It prevents cross conduction and allows ZVS. The converter has got four modes of operation during one switching period T_s. Before t_0, the switches S_2 and S_3, and the output diode D_{o1} are conducting. At t_0, the magnetizing current i_m and the secondary current i_s arrive at their minimum values I_{m2} and $-I_{Do1}$, respectively.

In mode 1, at t_0, the switches S_2 and S_3 are turned OFF. Then, the energy stored in the magnetic components starts to charge/discharge the parasitic capacitances C_1 through C_4. Therefore, the voltages v_{S2} and v_{S3} start to rise from zero. Similarly, the voltage v_{S4} starts to fall from $V_{in}+V_c$ and the voltage v_{S1} starts to fall from Vin. Since all the parasitic output capacitances C_1 through C_4 are very small, this transition time interval is very short and it is ignored in Fig. 3. When the voltages v_{S1} and v_{S4} arrive at zero, their body diodes D_1 and D_4 are turned ON. Then, the gate signals are applied to the switches S_1 and S_4. Since the currents have already flown through D_1 and D_4 and the voltages v_{S1} and v_{S4} are clamped as zero before the switches S_1 and S_4 are turned ON, zero-voltage turn-ON of S_1 and S_4 is achieved. With the turn-ON of S_1 and S_4, the primary voltage v_p across L_m is V_{in}. In mode 2, At t_1, the currents i_s and i_{Do1} arrive at zero and the diode D_{o1} is turned OFF. Then, the output diode D_{o2} is turned ON and its current increases linearly. Since the current changing rate of D_{o1} is controlled by the serial inductor L_s, its reverse-recovery problem is significantly alleviated. In mode 3, similar to mode 1, the switches S_1 and S_4 are turned OFF at t_2. The parasitic capacitors C_1 and C_4 start to be charged from zero, whereas the parasitic capacitors C_2 and C_3 start to discharge from V_{in} and V_{in} + V_c, respectively. After the parasitic capacitors are fully charged and discharged, the voltages v_{S2} and v_{S3} become zero and the body diodes D_2 and D_3 are turned ON. Then, the gate signals are applied to the switches S_2 and S_3. Since the currents have already flown through D_2 and D_3 and the voltages v_{S2} and v_{S3} are clamped as zero, zero-voltage turn-ON of S_2 and S_3 is achieved. In mode 4, similar to mode 2, the currents i_s and i_{Do2} arrive at zero and the diode D_{o2} is turned OFF at t_3. Then, the output diode D_{o1} is turned ON and its current increases linearly. Since the current changing rate of D_{o2} is controlled by L_s, its reverse-recovery problem is significantly alleviated[6].

The clamping capacitor voltage Vc is obtained by

$$V_c = \frac{2D-1}{1-D}V_{in} \quad (1)$$

The voltage gain M of the proposed converter is obtained by

$$M = \frac{V_0}{V_{in}} = \frac{n(1-2k)D}{(D-(1-2D)k)(1-D-(1-2D)k)} \quad (2)$$

Where

$$k = \frac{1}{2}\left(1-\sqrt{1-\frac{8L_sI_0}{nDV_{in}T_s}}\right) \quad (3)$$

$Also, d_1 = kD$ (4)

$d_2 = k(1-D)$ (5)

Fig 4 shows voltage gain M versus duty cycle D for various turns ratio n and keeping value of k as 0.06.

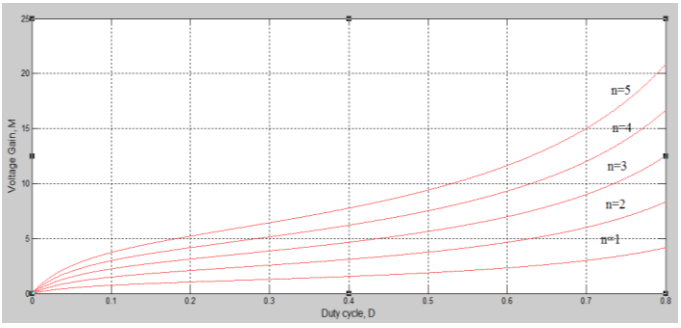

Fig -4: Voltage gain M according to duty cycle D

ISSN: 2250-3676
Volume-3, Issue-3, 217-223

The boundary condition for ZVS Conditions for the switches S_1 through S_4 is discussed below. From fig. 3, there is no current cancellation between i_p ($=ni_s$) and i_m at t_2. Therefore, for ZVS of S_2 and S_3 , the total energy stored in L_m and L_s should be larger than the energy stored in C_1 through C_4. Namely, the following condition should be satisfied:

$$\frac{L_m I_{m1}^2}{2}+\frac{L_s I_{D02}^2}{2}>\frac{(C_1+C_2)V_{in}^2}{2}+\frac{(C_3+C_4)(V_{in}+V_c)^2}{2} \quad (7)$$

Since n, I_{m1}, and I_{Do1} always have positive values and C_1 through C_4 are quite small. On the other hand, there is current cancellation between i_p ($= ni_s$) and i_m at t_0 . Therefore, for ZVS of $S1$ and $S4$, the energy difference between the energies stored in L_m and L_s should be larger than the energy stored in C_1 through C_4 as follows:

$$-\frac{L_m I_{m2}^2}{2}+\frac{L_s I_{D01}^2}{2}>\frac{(C_1+C_2)V_{in}^2}{2}+\frac{(C_3+C_4)(V_{in}+V_c)^2}{2} \quad (8)$$

3. MATHEMATICAL MODEL OF FUEL CELL

There are many mathematical model representing different fuel cell been developed over the years and one such mathematical equations representing a PEM fuel cell is discussed in this section[9]. The cell potential (V_{cell}), at any instance could be found using Eq. (9). When a cell delivers power to the load, the no-load voltage (E), is reduced by three classes of voltage drop, namely, the activation (V_{act}), ohmic (V_{ohm}), and concentration (V_{conc}) over voltages.

$$V_{cell}=E-V_{act}-V_{ohm}-V_{conc}\ \text{V} \quad (9)$$

The Nerst equation (Eq. 10) gives the open circuit cell potential (E) as a function of cell temperature (T) and the reactant partial pressures.

$$E=E_0-0.85\text{X}10^{-3}(T-298.15)+\frac{RT}{2F}\ln\left(\frac{P_{H_2}P_{O_2}^{0.5}}{P_{H_2O}P^{0.5}}\right) \quad (10)$$

Where E_0 represents the reference potential at unity activity, R is the universal gas constant and P is the total pressure inside the stack. F is the Faraday's constant.

The activation drop can be analyzed by Tafel's equation and the activation voltage drop (E_{act}) is given by

$$E_{act} = -0.9514 + 0.00312T - 0.000187T[\ln(I)] + 7.4\text{x}10^{-5}T[\ln(CO_2)]\ \text{V} \quad (11)$$

Where I (mA.cm-2) is the cell current density, the oxygen concentration(CO_2) is given as a function of stack temperature in Eq. (37)

$$CO_2=\frac{P_{O_2}}{5.08\text{X}10^6\exp(-498/T)}\ \text{mol.cm}^3 \quad (12)$$

Since, the activation overvoltage appears as a voltage drop in Eq. (11) and E_{act} in Eq. (13) is negative throughout the whole range, Eq. (38) is used to avoid a double negation for this term.

$$V_{act}=-E_{act}\ \text{V} \quad (13)$$

The effects of double layer capacitance charging at the electrode-electrolyte interfaces can be expressed by Eq. (14)

$$\frac{dV_{act}}{dt}=\frac{1}{C_{dl}}-\frac{V_{act}}{R_{act}C_{dl}} \quad (14)$$

Here C_{dl} is the double layer capacitance and R_{act} is the activation resistance, found by,

$$R_{act}=\frac{V_{act}}{I}\ \text{k}\Omega.\text{cm}^2 \quad (15)$$

It should be noted that, here, R_{act} stands for the effective resistance for a given cell current, I, and contributes to the activation overvoltage, V_{act}. On the other hand, Eq (14) is used to determine V_{act} at any instance of time. Therefore, these equations need to be used separately and cannot be interchanged. At intermediate current densities the voltage drop is almost linear and ohmic in nature. Membrane resistance (R_{mem}) is found by dividing the thickness, t_m, by the membrane conductivity, σ ($\text{k}\Omega^{-1}\text{cm}^{-1}$).

$$V_{ohm}=IR_{mem} \quad (16)$$

$$\text{Where } R_{mem}=\frac{t_m}{\sigma}\ \text{k}\Omega.\text{cm}^2 \quad (17)$$

The membrane water content depends on various factors, such as water drag from the anode to the cathode due to moving protons, external water content of the reactants, and back diffusion of water from the cathode to the anode. Since the effect of water drag is a significant factor, it could be hypothesized that the membrane proton concentration is a function of the cell current density only. An empirical differential equation could be solved to determine the proton concentration, C_{H+}, and Eq. (18) and (19) could be used to estimate the membrane conductivity, σ.

$$\frac{dC_{H_+}}{dt}+\frac{C_{H_+}}{\tau_{H_+}}=\frac{1+\alpha_{H_+}I^3}{\tau_{H_+}} \quad (18)$$

$$\sigma=\frac{F^2}{RT}D_{H_+}C_{H_+} \quad (19)$$

At higher current densities, the cell potential decreases rapidly due to mass-transport limitations. This linearity is termed as the concentration over potential and modeled as;

$$V_{conc}=a.e^b\ \text{V} \quad (20)$$

Here, the coefficient a (V), and b ($\text{cm}^2\ \text{mA}^{-1}$) vary with temperature and given as;

$$a = 1.1\text{x}10^{-4} - 1.2\text{x}10^{-6}(T-273)$$
$$b = 8\text{x}10^{-3}$$

Eq. (9)-(20) could be solved for cell potential, V_{cell}, as a function of current density, cell temperature, reactant pressure, and membrane hydration. If all the cells are in series, stack output is the product of cell potential and number of cells in the stack (N).

$$V_{stack}=V_{cell}xN \quad (21)$$

It is assumed that reactant flow at the anode and cathode is laminar, that the inlet gases are saturated at the given cell temperature. Assuming that all the gases are ideal, the ideal gas law could be extended for dynamic analysis and the principles of mole conservation could be used to

ISSN: 2250-3676
Volume-3, Issue-3, 217-223

model the reactant flows with the general equation given below;

$$\frac{V}{RT}\frac{dP_g}{dt} = m_{in} - m_{out} \pm \frac{I}{nF} \quad (22)$$

Where V is the anode or cathode volume (m^3), P_g is the gas (oxygen, hydrogen or vapor) pressure (atm), m_{in} is the reactant inlet flow rate (mol.s-1), m_{out} is the reactant outlet flow rate (mol.s-1), n is the number of electrons involved for each mole of reactant. To determine instantaneous conditions inside the cell, the conservation of gas reactants are calculated using the following formulas.

Anode flow model equations:

$$\frac{V_a}{RT}\frac{dP_{H_2}}{dt} = m_{H_2in} - m_{H_2out} - \frac{I}{2F} \quad (23)$$

$$m_{H_2out} = k_a(P_{H_2} - P_{amb})$$

$$m_{H_2in} = FRPC_{H_2}CF_{H_2}$$

Cathode flow model equations:

$$\frac{V_c}{RT}\frac{dP_{O_2}}{dt} = m_{O_2in} - m_{O_2out} - \frac{I}{4F} \quad (24)$$

$$m_{O_2out} = k_c(P_{O_2} - P_{amb})$$

$$m_{O_2in} = FRPC_{O_2}CF_{O_2}$$

$$\frac{V_c}{RT}\frac{dP_{H_2O\_C}}{dt} = m_{H_2O\_in\_C} - m_{H_2O\_out\_C} - \frac{I}{2F} \quad (25)$$

$$m_{H_2O\_out\_C} = k_c(P_{H_2O\_C} - P_{amb})$$

$$m_{H_2O\_in\_C} = FRPC_{H_2O\_C}$$

Where P_{amb} is the ambient temperature, V_a is the anode volume, k_a is the anode flow constant, V_c is the cathode volume, k_c is the cathode flow constant, PC_{H_2} is the percentage of hydrogen purity, CF_{H_2} is the hydrogen flow rate, PC_{O_2} percentage of oxygen purity, CF_{O_2} is the oxygen flow rate conversion factor, $PC_{H_2O\_C}$ is the cathode vapour content.

In the paper, the fuel cell is modelled using the above eqns and interfaced with asymmetrical full bridge converter ie, fuel cell is made as the dc source of the converter as shown in the below block diagram.

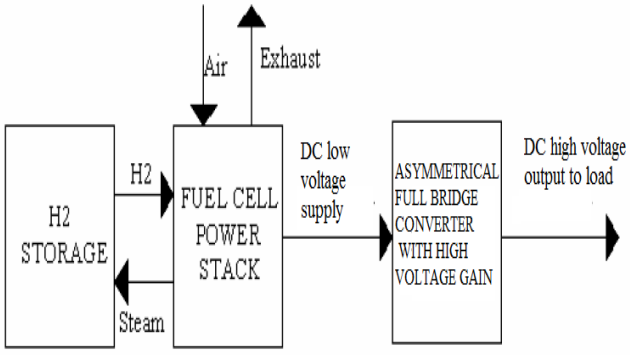

Fig-5: Asymmetrical FB converter with fuel cell as the source

4. COMPUTER SIMULATION AND RESULTS

The converter of Fig.1 is simulated using MATLAB/SIMULINK for the following input and output data specifications.

1) input voltage, V_{in}: 48V;
2) output voltage,V_o: 400V;
3) full-load power,P_{out}: 150:
4) switching frequency,f_s : 74 kHz.

As per the analysis, the voltage gain is 8.3 and turns ratio of 3 and L_s(130µH) and L_m (85µH). Using the mathematical eqns (9)-(22), the PEM fuel is modelled using Matlab/Simulink. The simulink model is shown in fig 6. where V_{cell} is the fuel cell voltage and is found to be 0.7V. The subsystem showing the mathematical model of E_{act} is also shown in fig 7. The fuel cell simulated output voltage V_{cell} is shown in fig 8.

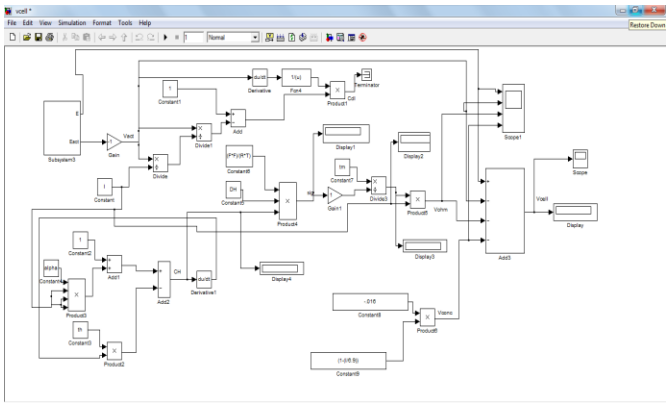

Fig-6: Matlab/Simulink model of PEM fuel cell

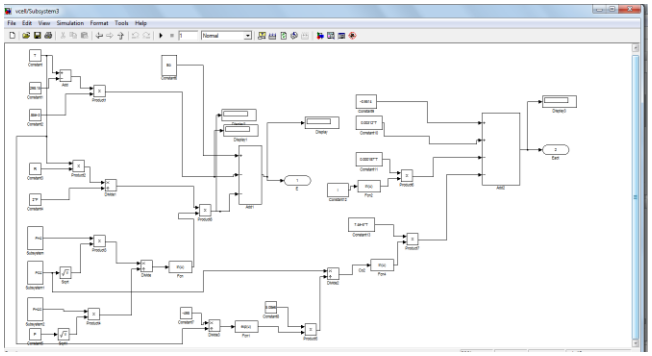

Fig-7: Subsystem showing Matlab/Simulink model of E_{act}

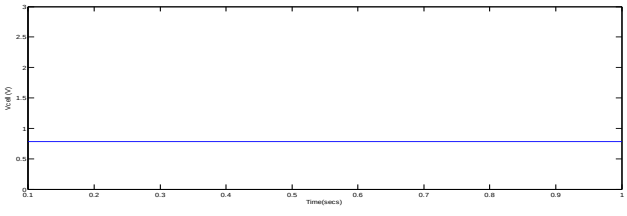

Fig-9: Output voltage the PEM fuel cell, V_{cell}

The simulated circuit diagram of the converter with fuel cell as its source is shown in fig 10. Fig 11 shows the stack voltage of the fuel cell. The output voltage and output current waveforms are shown in fig 12 and fig 13.

ISSN: 2250-3676
Volume-3, Issue-3, 217-223

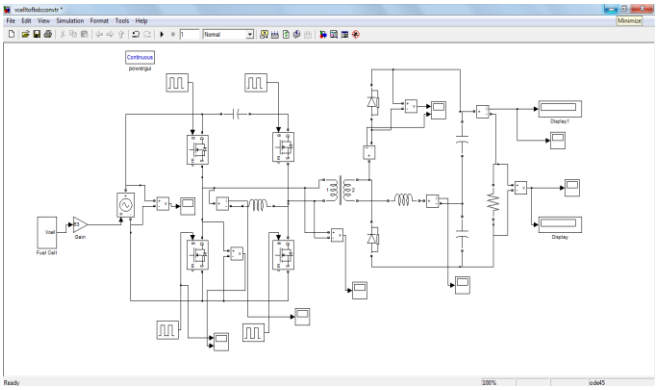

Fig-10: Simulated circuit diagram the Asymmetrical full bridge converter with fuel cell as dc source

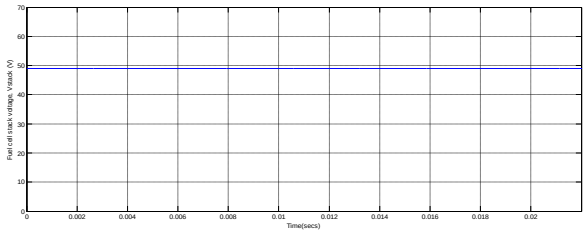

Fig-11: Waveform of fuel cell stack voltage which is input supply to asymmetrical dc-dc converter

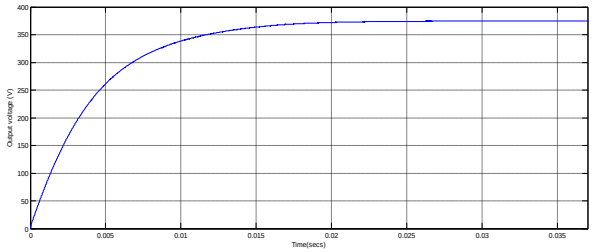

Fig-12: Output voltage

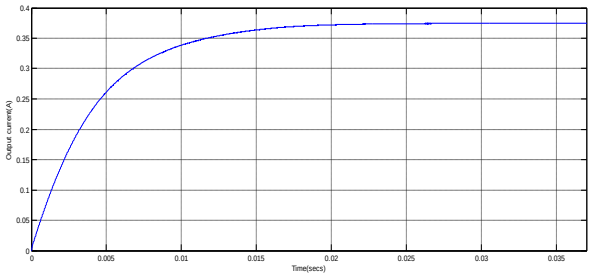

Fig-13: Output current

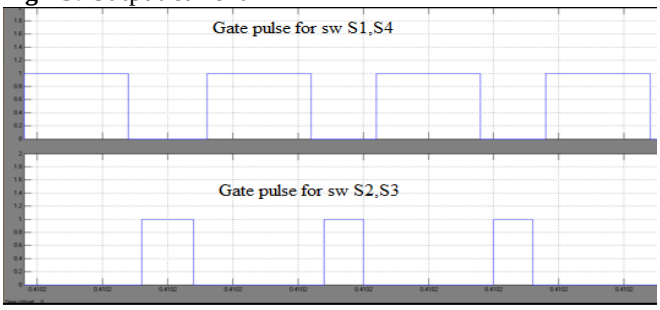

Fig-14: Waveform of driving pulses

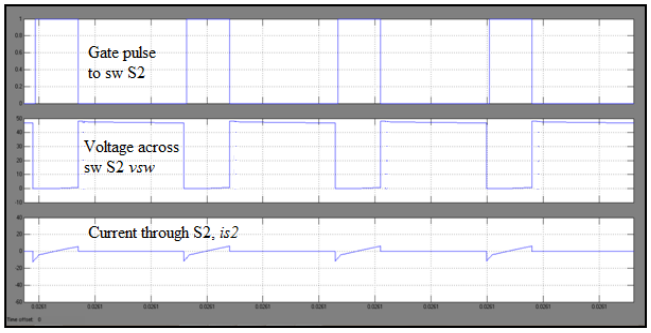

Fig-15: Waveforms showing gate pulse to switch S_2, voltage across switch S_2 and current flowing through it.

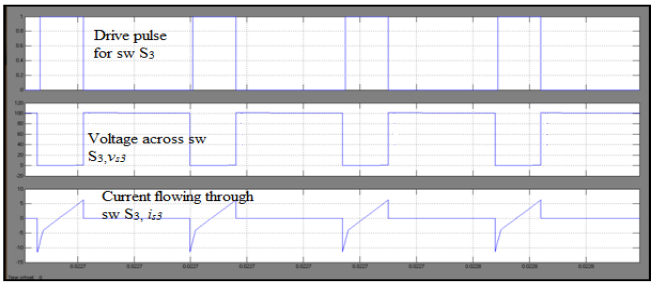

Fig-16: Waveforms showing gate pulse to switch S_3, voltage across switch S_3 and current flowing through it.

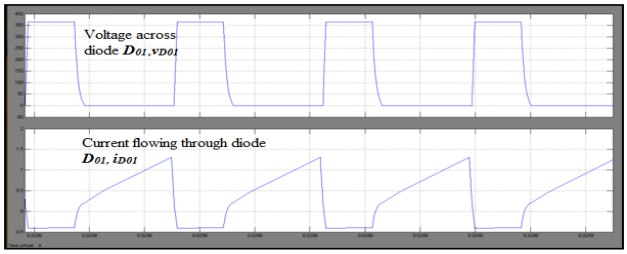

Fig-17: Waveforms showing voltage across and current flowing through, diode D_{01}

The driving pulses to switches and the voltage across and current flowing through switches and diodes are shown in figs 14-17. Its clear from the waveforms that the switches achieves ZVS and diodes ZCS.

5.CONCLUSION

In this paper, the asymmetrical full bridge converter with high voltage gain is interfaced with a PEM fuel cell. The ZVS of all power switches and ZCS of the output diodes are achieved. The converter is able to provide a high efficiency and high-voltage gain with relatively low transformer turns ratio.

REFERENCES

[1].N. Mohan , T. M. Undeland, W. P. Robbins, Power Electronics: Converters, Applications, and Design, *3rd Bk&Cdr edition*, Wiley, 2002.

[2].L.-S. Yang, T.-J. Liang, and J.-F. Chen, "Transformerless DC-DC converters with high step-up voltage gain," *IEEE Trans. Ind. Electron.*, vol. 56, no. 8, pp. 3144–3152, Aug. 2009.

ISSN: 2250-3676
Volume-3, Issue-3, 217-223

[3].A. J. Zhang, G. Huang, and Y. Gu, "Asymmetrical full bridge DC-to-DC converter," U.S. Patent 6 466 458, Oct. 15, 2002.
[4].P. Imbertson and N. Mohan, "Asymmetrical duty cycle permits zero switching loss in PWM circuits with no conduction loss penalty," *IEEE Trans. Ind. Appl.*, vol. 29, no. 1, pp.121–125, Jan./Feb. 1993.
[5].A. Fiedler and H. Grotstollen, "Investigation of asymmetrical phaseshifted full bridge," in *Proc. IEEE IECON*, 1995, pp. 434–439.
[6].Hyun-Lark Do, "Asymmetrical Full-bridge Converter With High-Voltage Gain" *IEEE Trans. Power Electron*, vol. 27, no. 2, february 2012
[6].Ken Stanton, Jih-Sheng (Jason) Lai, and Douglas Nelson, "Dynamic PEM Fuel Cell Model for Power Electronics Design with Temperature Consideration"
[7].K. Sedghisigarchi and A. Feliachi, "Dynamic and Transient Analysis of Power Distribution Systems With Fuel Cells-Part I: Fuel-Cell Dynamic Model," *IEEE Trans. Energy Conv.*, Vol. 19, no. 2, pp. 423-428, June 2004.
[8].Bouziane Mahmah, Abdelhamid M'raoui, Maïouf Belhamel, Hocine Benmoussa,"Experimental Study and Modelling of a Fuel Cell PEMFC Fed Directly with Hydrogen / Oxygen",2006.
[9]. Zehra Ural1, Muhsin Tunay Gencoglu and Bilal Gumus, "Dynamic Simulation of a Pem Fuel Cell System" *Proceedings* 2nd International Hydrogen Energy Congress and Exhibition IHEC 2007 Istanbul, Turkey, 13-15 July 2007.

BIOGRAPHIES

Divya S, received B-Tech from Toch Institute of Science and Technology, India in 2008. She is currently doing her M-Tech in Power Electronics and Control at Govt,Engineering College, Idukki, India

Sreedevi G, reciecved B-Tech and M-Tech from College of Engineering, Thiruvanthapuram, India. She has worked as Assistant Engineer in Kerala State Electricity Board. She currently working as Assistant professor in Govt,Engineering College, Idukki, India.